

# Experimental demonstration of Epsilon-Near-Zero water waves focusing

T.Bobinski<sup>1</sup>, A.Eddi<sup>1</sup>, A.Maurel<sup>2</sup>, V.Pagneux<sup>3</sup> and P.Petitjeans<sup>1</sup>

<sup>1</sup>Laboratoire de Physique et Mécanique des Milieux Hétérogènes (PMMH), UMR CNRS 7636-ESPCI-UPMC Univ. Paris 6-UPD Univ. Paris 7, 10 rue Vauquelin, 75005 Paris, France

<sup>2</sup>Institut Langevin LOA, UMR CNRS 7587-ESPCI, 5 rue Jussieu, 75005 Paris, France

<sup>3</sup>Laboratoire d'Acoustique de l'Université du Maine, UMR CNRS 6613, Avenue Olivier Messiaen, 72085 Le Mans, France

Email: tomasz.bobinski@espci.fr

## Highlights

We investigate experimentally  $\epsilon$ -near-zero (ENZ) analogue for water waves in nonlinear regime by tuning bathymetry of the system. We obtain uniform phase at the edge of a semi circular lens, resulting in expected lensing effect. Two-dimensional time space measurements of the surface elevation allow us to separate the linear component and harmonics generated due to nonlinearities. The origin of the harmonics is analyzed in the frame of the competition between free-waves and bound-waves. The results show dominance of free-waves. Surprisingly, we observe a cascade of sub wavelength focal spots with respect to the first harmonic.

## 1 Introduction

One of the group of newly-designed metamaterials is the so-called  $\epsilon$ -near-zero materials. In the context of electromagnetic wave, medium filled with such material can be characterized by a very large wavelength. This property makes tailoring phase pattern feasible. Using a semi circular shape at the output of ENZ material, one can obtain extremely well focused wave at the center of such lens. Two-dimensional electromagnetic wave in transverse magnetic polarization can be described by the following equation:

$$\nabla \left( \frac{1}{\epsilon} \nabla H \right) + \frac{\omega^2}{c_0^2} H = 0. \quad (1)$$

with  $H$  the magnetic field,  $\omega$  is the frequency,  $c_0$  is the light speed in vacuum and  $\epsilon$  is the permittivity. As  $\epsilon$  approaches zero value, refractive index tends to vanish. This allows to achieve constant phase throughout the medium.

In the context of water waves, the ENZ analogy can be analyzed by first considering shallow water approximation:

$$\nabla (h \nabla \eta) + \frac{\omega^2}{g} \eta = 0 \quad (2)$$

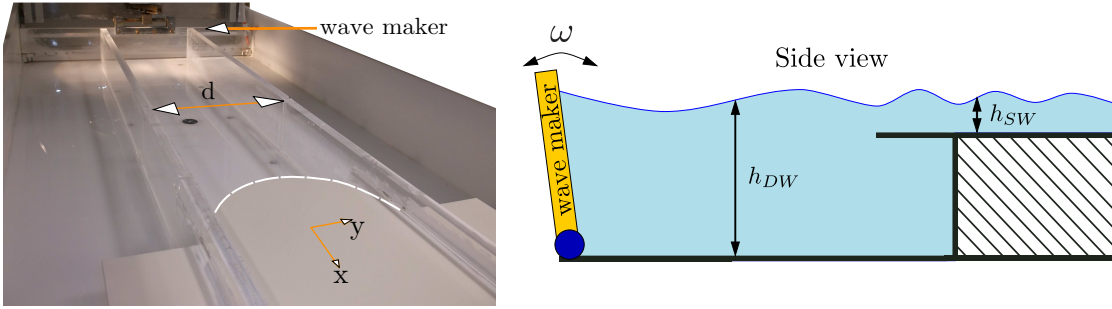


Figure 1: Experimental setup. Position of the lens is marked with white dashed line.

where  $h$  denotes the water depth at rest and  $g$  stands for the gravitational acceleration. In this regime, wavenumber is given as  $k_{SW} = \omega/\sqrt{gh}$ . By comparing Eqs.(1) and (2), one obtains correspondence of permittivity for water waves, i.e.  $1/\epsilon \leftrightarrow h$ , indicating that the ENZ can be realized in water waves system for  $h^{-1}$ -near-zero. By increasing depth, we end up with deep water approximation for which wavenumber is given as  $k_{DW} = \omega^2/g$ . Therefore, the efficiency of the  $h^{-1}$ -near-zero is given through refractive index defined as  $n = k_{SW}/k_{DW} = \sqrt{g/\omega^2 h}$ .

## 2 Experimental arrangements

Our system consists of a lens inside a waveguide. The lens is a semi circular edge of diameter  $d = 20\text{cm}$ . The width of the waveguide is adjusted to the size of the lens. The lens is a boundary between two regions with different depths. Depth in a shallow water part (behind the lens) is set to  $h_{SW} = 7\text{ mm}$ , while in a deep water region it is  $67\text{ mm}$ . Waves are generated by a paddle wave maker working within a frequency range  $\omega \in [6.28; 13.19]\text{ s}^{-1}$ , which is shown together with the experimental setup in Fig. 1. We perform time space resolved measurements of the surface elevation using Fourier Transform Profilometry method adapted by our team for water wave measurements [2, 3]. We project fringes by means of a high-resolution projector ( $1920 \times 1080\text{pix}^2$ ). Images are recorded using 4MPix camera with sampling frequency 15Hz. The area of interest is  $0.4 \times 0.2\text{ m}^2$  large and covers deep and shallow water regions.

## 3 Results and analysis

As expected, in the deep water region wave has a almost constant phase and focuses in shallow water region. As shallow water waves are easily nonlinear, we give the measure of nonlinearity by Ursell number, which in our case is typically of order  $U_r = 378$ . Hence, we investigate strongly nonlinear case. Temporal spectrum, determined at the center of the lens, indicates the magnitude of second harmonic which is 30% of the fundamental component, while higher-order terms remain significant.

Temporal decomposition of the obtained surface elevation fields allows us to separate the influence of each of harmonics. We suppose that surface elevation  $\eta$  can be expressed as:

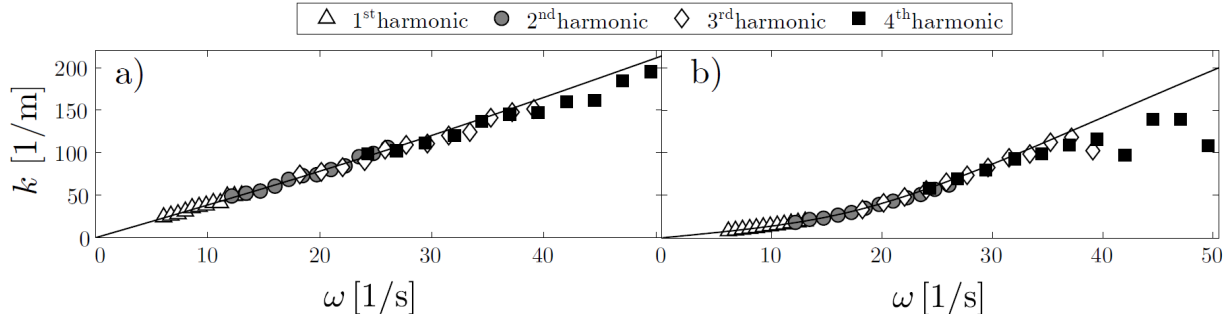


Figure 2: Measured dispersion relation in: a) shallow-water region and b) deep-water region. Solid lines correspond to linear dispersion relation in both regions.

$$\eta(x, y, t) = \sum_{n=0}^N \hat{\eta}_n(x, y) \exp(in\omega t) \quad (3)$$

where  $\hat{\eta}_n(x, y)$  denote complex field corresponding to the  $n$ -th harmonic of the fundamental pulsation  $\omega$ . We extract  $\hat{\eta}_n$  using Fast Fourier Transform.

To describe nature of the harmonics we consider two different types of waves related to nonlinear regime, i.e. bound-waves and free-waves. We can discriminate them because of the difference in dispersion relation. Wavenumber related to free-waves can be described as  $k = D(n\omega)$ , whereas bound-waves indicate relation  $k = nD(n\omega)$ . To determine dispersion relation in our experiments we first consider inhomogeneous Helmholtz equation. Neglecting source terms [1], appearing due to nonlinearities, yields the homogeneous problem corresponding to free-waves:

$$(\Delta + \mathbf{k}_n^2) \hat{\eta}_n(x, y) = 0 \quad (4)$$

where  $\mathbf{k}_n$  is linked to  $n\omega$  through the linear dispersion relation. To calculate wavenumber  $\mathbf{k}_n$  from a given complex pattern  $\hat{\eta}_n(x, y)$ , the norm function  $\|(\Delta + \mathbf{k}_n^2) \hat{\eta}_n\|$  is minimized in the complex plane  $\mathbf{k}_n$  [4]. We determine wavenumbers in the far-field of deep and shallow-water regions separately. By applying described procedure we obtain  $k$  for the first and higher harmonics. Measured dispersion relation for all of the components is presented in Fig. 2a),b). In shallow-water part results are in agreement with linear dispersion relation. This confirms that harmonics are dominated by free-waves rather than bound-waves.

Having the nature of harmonics described, we are interested in the quality of the obtained focusing, which is presented in Fig. 3. We show the total field, defined as  $I(x, y) = \max_{t \in [0, T]} \eta^2(x, y, t)$ , and the intensity fields  $I_n(x, y) = |\hat{\eta}_n(x, y)|^2$  (normalized by the maximum intensity value of each term  $\max I_n$ ) corresponding to first four harmonics. Surprisingly, each successive  $n$ -th harmonic is characterized by more and more focused spot. Shape of the focal spot differs among harmonics. The lateral size of the focal spot is decreasing for higher-order terms, meanwhile the horizontal extension remains almost constant. We determine the efficiency of the lens by the following quantities: (i) axial and lateral extension of the focal spot  $L_x$  and  $L_y$ , (ii) axial position of the maximum intensity  $X$ , and (iii) contrast of the focal spot  $A_{max}/\bar{A}$ . The results indicate that  $L_x/\lambda_{sw}$ , with  $\lambda_{sw}$  being

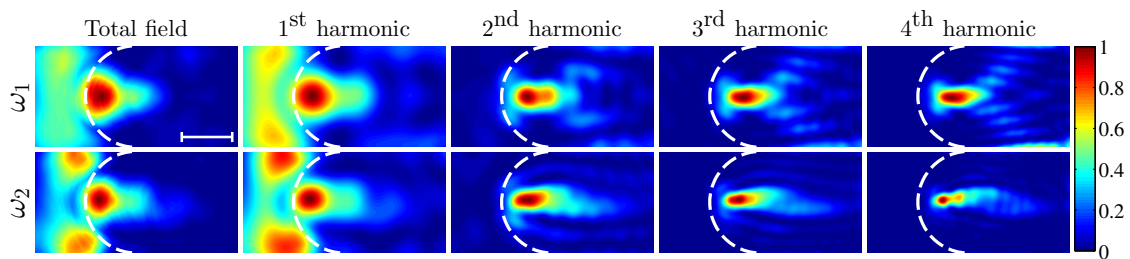


Figure 3: Normalized intensity of the wave field ( $I/I_{max}$ ) for  $\omega_1 = 9.86 \text{ s}^{-1}$  and  $\omega_2 = 12.39 \text{ s}^{-1}$ . White dashed line marks the position of the lens. Scale bar in the left top figure corresponds to 0.1 m.

wavelength in shallow water region, varies slowly with the pulsation, while  $L_y/\lambda_{sw}$  follows expected scaling law  $\lambda/2$ .

## 4 Conclusions

Characteristic property of the ENZ metamaterials is their incredibly high value of phase velocity, resulting in almost constant phase through a medium. Theoretically, this should allow to perfectly focus waves at a single point. Due to intrinsic properties of water waves one has to face constraints, which do not allow to obtain similar phase velocities. The limitation is governed by the deep-water approximation. Nevertheless, our experiments illustrate that thanks to ENZ analogy it is possible to focus water waves efficiently. With large amplitude of an incident wave we obtained surprising cascade of highly focused nonlinear components.

## References

- [1] K.A. Belibassakis and G.A. Athanassoulis. A coupled-mode system with application to nonlinear water waves propagating in finite water depth and in variable bathymetry regions. *Coastal Engineering*, 58(4):337–350, April 2011.
- [2] P. J. Cobelli, A. Maurel, V. Pagneux, and P. Petitjeans. Global measurement of water waves by fourier transform profilometry. *Experiments in Fluids*, 46(6):1037–1047, June 2009.
- [3] A. Maurel, P. Cobelli, V. Pagneux, and P. Petitjeans. Experimental and theoretical inspection of the phase-to-height relation in fourier transform profilometry. *Applied Optics*, 48(2):380–392, 2009.
- [4] A. Prządka, B. Cabane, V. Pagneux, A. Maurel, and P. Petitjeans. Fourier transform profilometry for water waves: how to achieve clean water attenuation with diffusive reflection at the water surface? *Experiments in Fluids*, 52(2):519–527, February 2012.